

LARGE-SCALE NUMERICAL SIMULATIONS ON TWO-PHASE FLOW BEHAVIOR IN A FUEL BUNDLE OF RMWR WITH THE EARTH SIMULATOR

**Kazuyuki Takase¹, Hiroyuki Yoshida¹, Yasuo Ose²,
Hidesada Tamai¹ and Hajime Akimoto¹**

1 Japan Atomic Energy Research Institute, Tokai, Ibaraki, 319-1195, Japan

2 Yamato System Engineer, Hitachi, Ibaraki, 319-0063, Japan

Abstract

Fluid flow characteristics in a fuel bundle of a reduced-moderation light water reactor (RMWR) with a tight-lattice core were analyzed numerically using a newly developed two-phase flow analysis code under the full bundle size condition. Conventional analysis methods such as sub-channel codes need composition equations based on the experimental data. In case that there are no experimental data regarding to the thermal-hydraulics in the tight-lattice core, therefore, it is difficult to obtain high prediction accuracy on the thermal design of the RMWR. Then the direct numerical simulations with the earth simulator were chosen. The axial velocity distribution in a fuel bundle changed sharply around a grid spacer and its quantitative evaluation was obtained from the present preliminary numerical study. The high prospect was acquired on the possibility of establishment of the thermal design procedure of the RMWR by large-scale direct simulations.

Introduction

Although sub-channel codes [1]-[3] are used for the thermal-hydraulic analysis of fuel bundles in nuclear reactors from the former, many composition and empirical equations based on experimental results are needed to predict the two-phase flow behavior in details. When there are no experimental data such as the reduced-moderation light water reactor (RMWR) [4]-[6] which is studied by the Japan Atomic Energy Research Institute (JAERI), therefore, it is very difficult to obtain highly precise predictions.

The RMWR core has remarkably narrow gap spacing between fuel rods (i.e., around 1 mm) which are arranged at a triangular tight-lattice configuration in order to reduce the moderation of the neutron. In such a tight-lattice core, there is no sufficient information about the effects of the gap spacing and grid spacer configuration on the fluid flow characteristics. Then, the authors tried to analyze numerically on the thermal-hydraulics in a fuel bundle with grid spacers using large-scale direct simulations under the full bundle size condition.

Although lots of calculation memories are required to attain the direct numerical simulations for the RMWR fuel bundle, the earth simulator (ES) [7] in Japan enabled such a request. The ES is a highly parallel vector supercomputer system of the distributed-memory type, and consists of 5120 arithmetic processors with 10 TB of main memory and the theoretical performance of 40 Tflops.

The present study was carried out with a newly developed thermal-hydraulic analysis code for multi-phase flow. It can predict the two-phase behavior with the liquid-gas interaction in the time and space directions with high accuracy. This paper describes the results of the preliminary fluid flow analysis in just one fuel bundle of RMWR using the ES.

Outline of RMWR

RMWR Core Structure

The RMWR is a light water reactor with a higher conversion ratio than one by controlling the water flow rates. In order to get 1.0 or more conversion ratios, it is expected from the results of the previous studies that the volume ratio of water and fuel must be decreased to about 0.25 or less. To satisfy this condition, the fuel bundle with a triangular tight-lattice arrangement is required. Here, a fuel rod diameter is around 13 mm and the gap spacing between each rod is around 1 mm. Although the coolant is 100% water at the core inlet, it changes water and vapor along the flow direction, and then the vapor occupies 70% or more at the core outlet. The flow rate at the actual RMWR core is reduced down to around 10 % of the water flow rate at the BWR with 8x8 fuel rod bundle. Therefore, the RMWR has very severe cooling condition on the viewpoint of the thermal engineering.

Figure 1 shows a bird-eye view of the actual RMWR design. It consists of core, control rods, separator and dryer regions, and a pressure vessel. The pressure vessel diameter and height are around 9 and 19 m. The core region is composed of 282 fuel bundles as can be seen in Fig.2. The fuel bundle has a hexagonal shape horizontally. A length of one side of a hexagonal shape is about 0.13 m and the axial length of a fuel bundle is about 2.9m. A heating section in the core consists of the two seed and

three blanket regions and its length is about 1.3 m (i.e., around 0.2 m in each seed region and 0.3 m in each blanket region). In the core, MOX (mixed oxide) is used to the seed region and then the depleted UO_2 is used to the blanket region.

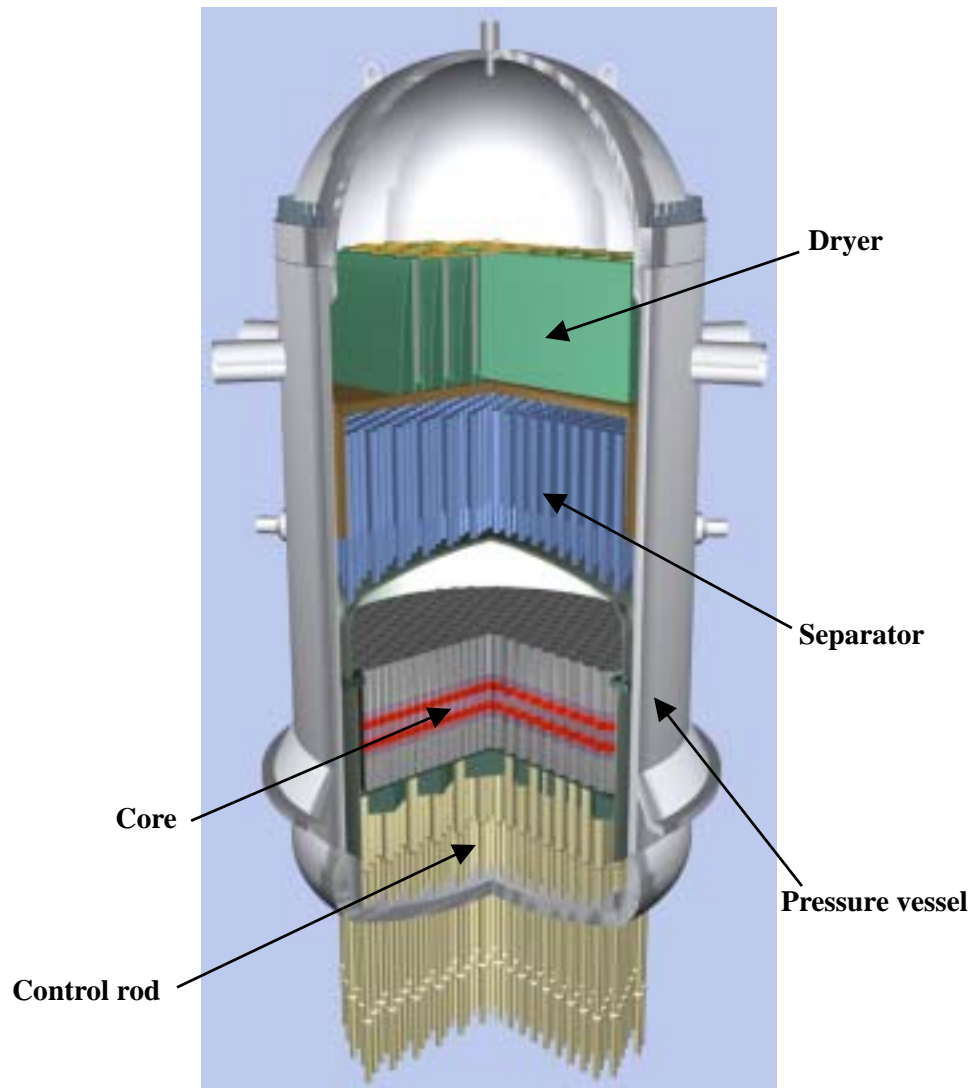


Fig. 1 Appearance of the RMWR

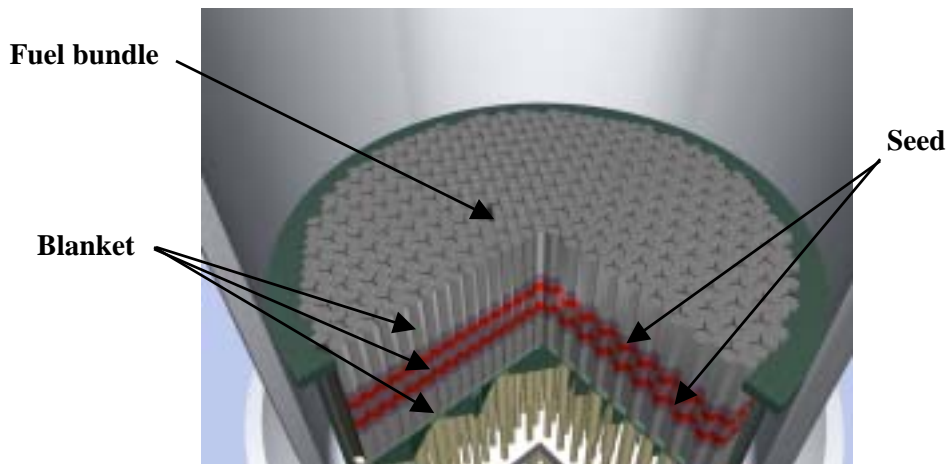


Fig.2 282 fuel bundles installed into a core region of the RMWR

Grid Spacer

The role of a grid spacer is as follows.

- 1) To keep the gap spacing between fuel rods, and
- 2) To restrict the movement of a fuel rod to the radial and circumferential directions.

The outline of the shape of a current designed grid spacer is shown in Fig. 3. Its shape is like a honeycomb. The grid spacer is installed around each fuel rod with a triangular tight-lattice arrangement in the horizontal direction. The fuel rod is supported by three spacer ribs, which are set to the inside of the grid spacer. These grid spacers are installed in several axial positions. Water flows from a perpendicular direction to Fig.3.

D: fuel rod diameter, g: gap spacing between fuel rods, t: thickness of a grid spacer

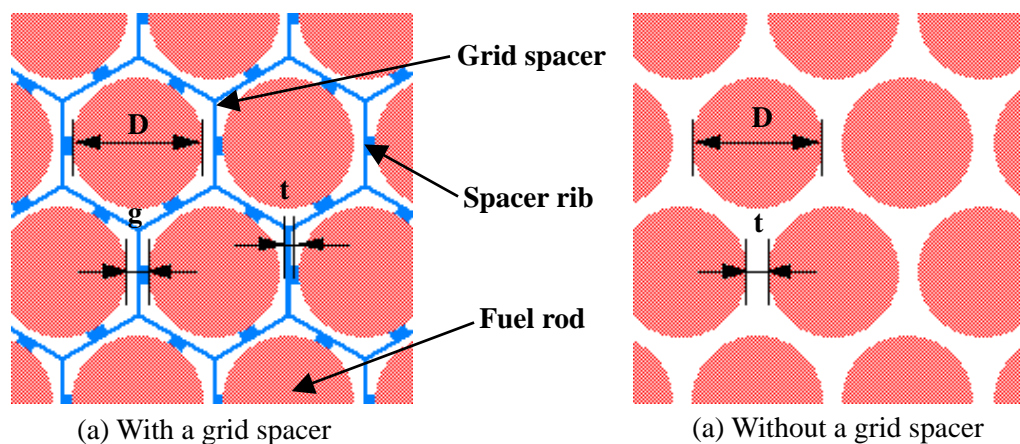


Fig.3 Layout of fuel rods with and without a grid spacer

Outline of Earth Simulator

The ES, which was developed as a national project of Japan by three governmental agencies, JAERI, the National Space Development Agency of Japan (NASDA), and Japan Marine Science and Technology Center (JAMSTEC). The ES is housed in the Earth Simulator Building (approximately 50m x 65m x 17m), as can be seen in Fig. 4. It is a highly parallel vector supercomputer system of the distributed-memory type, and consisted of 640 processor nodes connected by 640x640 single-stage crossbar switches. Each processor node is a system with a shared memory, consisting of 8 vector-type arithmetic processors, a 16-GB main memory system, a remote access control unit, and an input and output processor. The peak performance of each arithmetic processor is 8 Gflops. The ES as a whole thus consists of 5120 arithmetic processors with 10 TB of main memory and the theoretical performance of 40 Tflops.

Major objectives of the ES are as follows:

- 1) Quantitative prediction and assessment of variations of the atmosphere, ocean and solid earth;
- 2) Production of reliable data to protect human lives and properties from natural disasters and environmental destruction;
- 3) Contribution to symbiotic relationship of human activities with nature; and
- 4) Promotion of innovative and epoch-making simulation in any fields such as industry, bioscience, energy and so on.

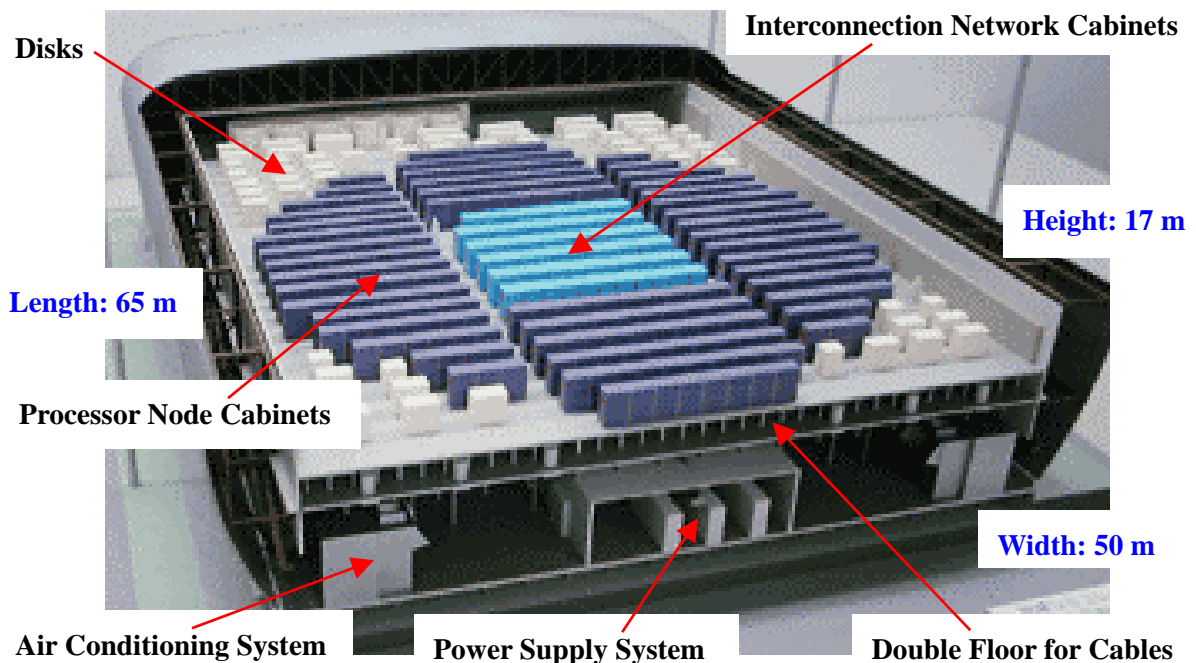


Fig.4 Appearance and composition elements of the ES

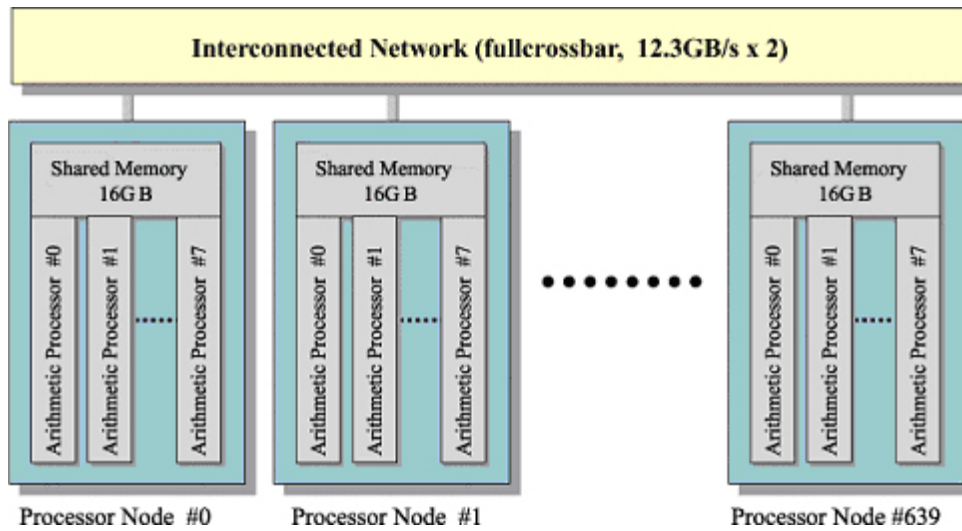


Fig.5 Outline of the interconnected network of the ES

Figure 5 shows an outline of the interconnected network constructed into the ES. The remote access control unit is directly connected to the crossbar switches and controls inter-node data communications at 12.3GB/s bidirectional transfer rate for both sending and receiving data. Thus the total bandwidth of inter-node network is about 8 TB/s. Several data-transfer modes, including access to three-dimensional sub-arrays and indirect access modes, are realized in hardware. In an operation that involves access to the data of a sub-array, the data is moved from one processor node to another in a single hardware operation, and relatively little time is consumed this processing.

Numerical Analysis

Analytical Method

The two-phase flow analysis code TPFIT developed by Yoshida [8] was used to the present numerical analysis. This code can transport an interface between the liquid and gas in the time and space directions with high accuracy. The TPFIT is discretized using the CIP method [9] based on the non-conservative fluid equations. In the CIP method, the density function in an interface is assumed to be continuous. With regard to this density function, the interface tracking is carried out by the digitizer function (i.e., tangent conversion). When the density function in an interface does not have consistency with the digitizer function or the small bubbles and droplets generate, therefore, there is a possibility that a part of bubbles and droplets may disappear. This is due to that the interface tracking procedure is not established enough yet.

Then, Yoshida improved a transportation method of the volume of fluid as the gradient of the interface proposed by Youngs [10] becomes consistent with the CIP method. As a result of this, a practical two-phase flow analysis with the CIP method was available. The surface tension is calculated using the continuum surface force (CSF) model proposed by Brackbill [11]. This model is added into a source term in the momentum conservation equation (3) as σ_i .

Governing Equations

The tracking of an interface between the liquid and gas phase is accomplished by the solution of a continuity equation for the volume fraction of a couple of the phases. The governing equations for the present two-phase flow analysis are written by:

$$\begin{aligned} \text{- Mass conservation,} \quad \frac{D\rho}{Dt} &= -\rho \frac{\partial u_i}{\partial x_i} \\ & \rho = \rho_l \phi_l + \rho_g \phi_g, \quad \phi_g = 1 - \phi_l \end{aligned} \quad (1)$$

$$\text{- Density function,} \quad \frac{D\rho_l \phi_l}{Dt} = -\rho_l \phi_l \frac{\partial u_i}{\partial x_i}, \quad \frac{D\rho_g \phi_g}{Dt} = -\rho_g \phi_g \frac{\partial u_i}{\partial x_i} \quad (2)$$

$$\text{- Momentum conservation,} \quad \frac{Du_i}{Dt} = -\frac{1}{\rho} \frac{\partial p}{\partial x_i} + \frac{1}{\rho} \frac{\partial \tau_{ij}}{\partial x_j} + g_i + \sigma_i \quad (3)$$

$$\text{- Energy conservation,} \quad \frac{De}{Dt} = -\frac{p}{\rho} \frac{\partial u_i}{\partial x_i} + \frac{1}{\rho} \frac{\partial}{\partial x_i} \left(\lambda \frac{\partial T}{\partial x_i} \right) + q \quad (4)$$

$$\text{- Volume fraction,} \quad \frac{D\phi_l}{Dt} = 0, \quad \frac{D\phi_g}{Dt} = 0 \quad (5)$$

Analytical Model and Boundary Conditions

Figure 6 shows the present analytical model. It consists of 37 fuel rods and a hexagonal flow passage which is a casing made of stainless steel. The geometry and dimensions simulate the 37-rod bundle heat transfer test facility [12],[13] that was constructed to obtain the critical heat flux data on triangular tight-lattice coolant channels in the RMWR core. The fuel rod outer diameter is 13 mm and the gap spacing between each rod is 1.3 mm. The casing has a hexagonal cross section and a length of one hexagonal side is 51.6 mm. An axial length of the fuel bundle is 1260 mm. The water flows upward from the bottom of the fuel bundle. A flow area is a region in which deducted the cross-sectional area of all fuel rods from the hexagonal flow passage. Grid spacers are installed into the fuel bundle at the axial positions of 220, 540, 750 and 1030 mm from the bottom. The axial length of each grid spacer is 20 mm.

Inlet conditions of water are as follows: temperature 288°C, pressure 7.2 MPa, flow rate 400 kg/m²s, and the estimated Reynolds number is 40,000. On the other hand, boundary conditions are as follows: fluid velocities for x, y and z directions are zero on every wall (i.e., an inner surface of the hexagonal flow passage and outer surface of each fuel rod, and surface of each grid spacer); At the inlet of the fuel bundle the velocity profile is uniform. The void fractions of water and vapor were varied. As the preliminary numerical study three-dimensional calculations were carried out under the non-heated isothermal flow condition in order to remove the effect of heat transfer by the fuel rods which affect the fluid flow characteristics. In the present analysis the non-uniform mesh division was applied and the present minimum and average mesh size were 0.01 and 0.3 mm.

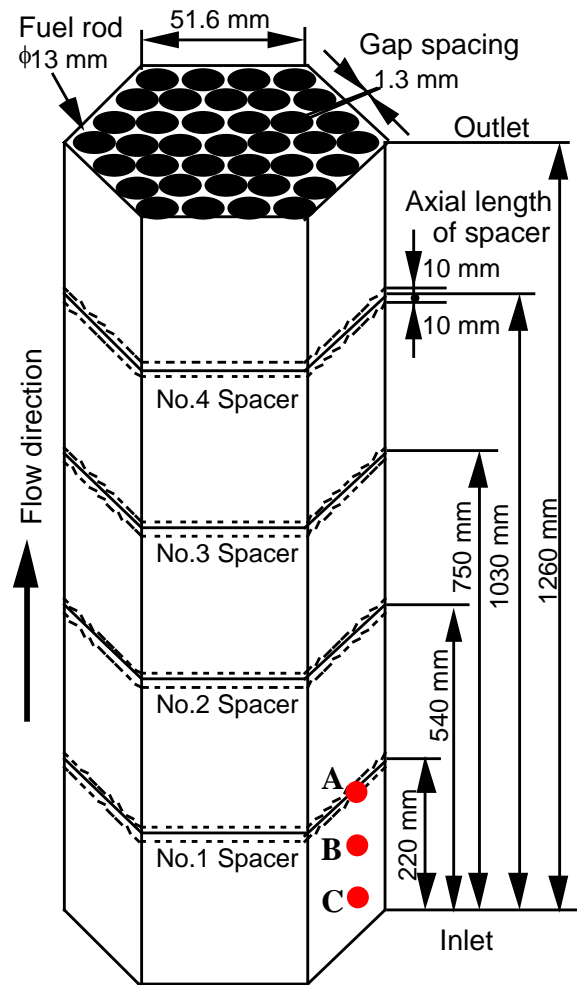


Fig.6 Analytical geometry and dimensions of a simulated RMWR fuel bundle with 37 fuel rods and four grid spacers

Analytical Results and Discussion

Predicted axial velocity distributions in three horizontal planes of the fuel bundle are shown in Fig. 7. Here, (a) shows the result of the position in front of a grid spacer, (b) is the result of the grid spacer position, and (c) is the result of the position just behind a grid spacer. Figure 7 (b) corresponds to the position A in Fig. 6. Then, white circles shown in Figs. 7 (a)-(c) represent fuel rods. The axial velocity is expressed using the color gradation: blue is 0 m/s in minimum and red is 0.8 m/s in maximum. The axial velocity is gradually accelerated in front of a spacer (Fig.7 (a)) and becomes the highest at the just spacer position (Fig.7 (b)), and it decreases from the highest value by sudden expansion of the flow channel behind a spacer, and then becomes 0.4-0.5 m/s at the core flow region (Fig.7 (c)). On the other hand, since the axial velocity approaches zero in the region in which touches the side wall of the flow channel, it becomes extremely low in comparison with that of the core flow region. Here, as can be seen in Fig.7 (b), the white line like a honeycomb between each fuel rod express a grid spacer.

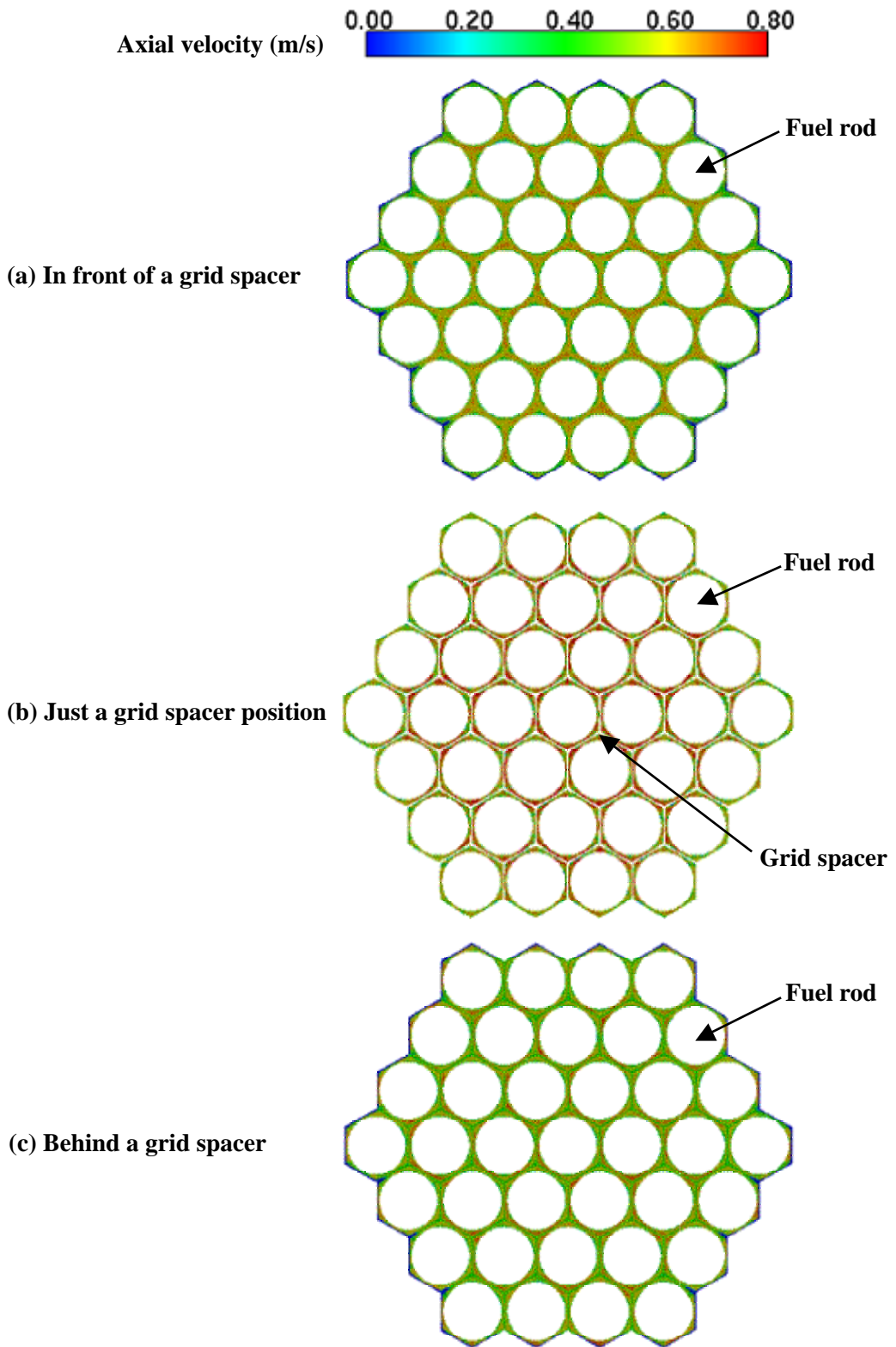


Fig.7 Cross-sectional views of predicted axial velocity distributions around a grid spacer corresponding to the position A in Fig. 6.

Figure 8 shows predicted axial velocity distributions near the position A in Fig. 6. Here, the regions in which the fuel rods are inserted are shown with space. Figure 8 (a) presents the result that looked at the upstream side from the downstream side of the flow channel. Figure 8 (b) is a cross-sectional view of the line D-D in Fig. 8 (a), and then, the lower position indicates the upstream side of the channel. A continuous change of the axial velocity through a grid spacer can be easily known. A red portion represents a higher axial velocity area in which was accelerated by reduction of a cross-sectional area in the flow channel. A higher velocity area shown by red and a lower velocity area shown by blue exist adjoining each other locally. It can be understood that reconstruction of the velocity distribution is performed in the positions before and behind a grid spacer.

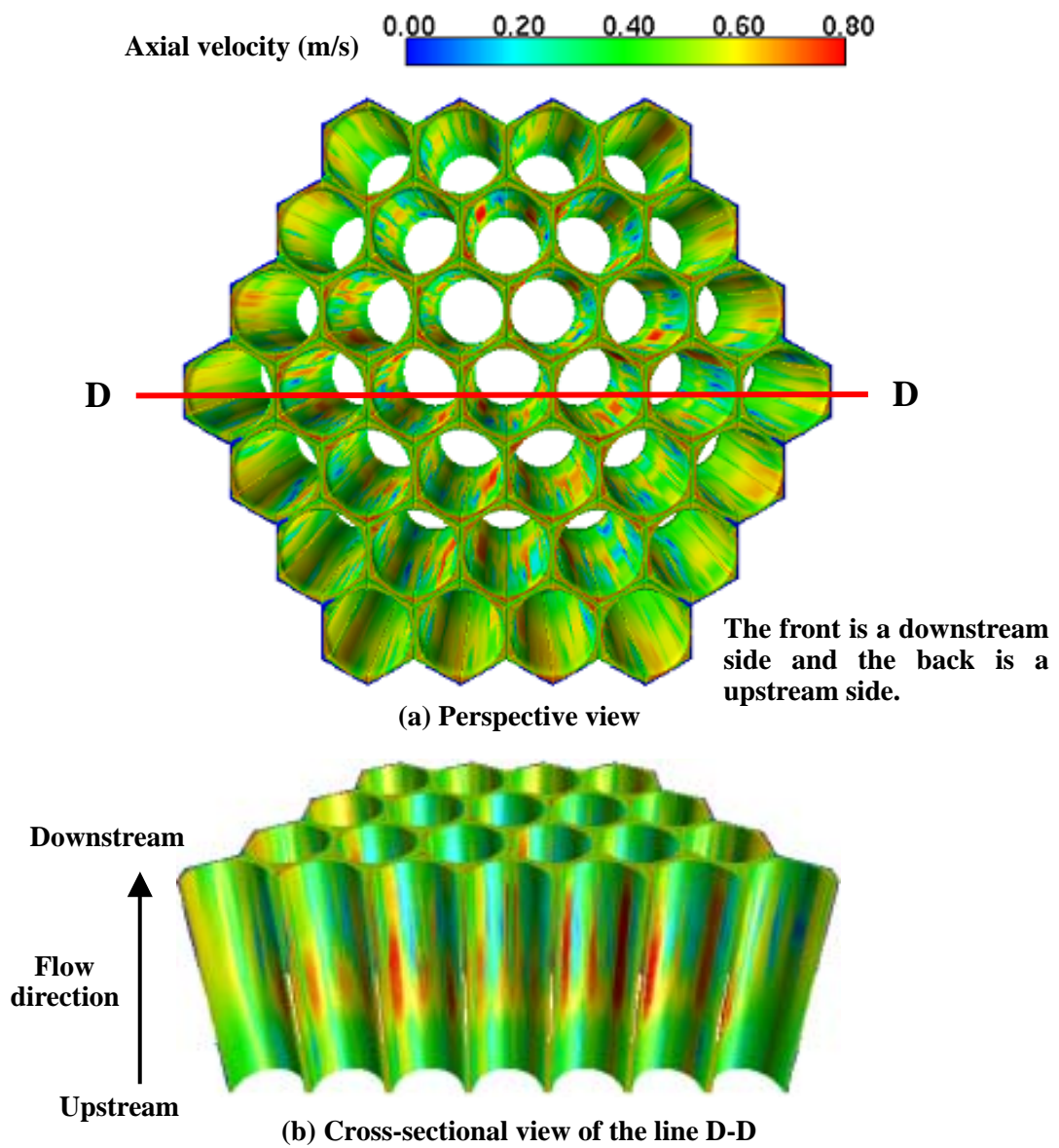


Fig.8 Predicted axial velocity distributions near the position A in Fig.6

Similarly, Fig. 9 shows predicted axial velocity distributions near the position B in Fig. 6. Figure 9 (a) represents the result that looked at the upstream side from the downstream side of the flow channel. Figure 9 (b) is a cross-sectional view of the line E-E in Fig. 9 (a). The influence of a grid spacer to the axial velocity is not seen in this axial position. The axial velocity, especially in a core flow region compared with a side wall region of the fuel bundle, develops gradually with increasing the axial distance.

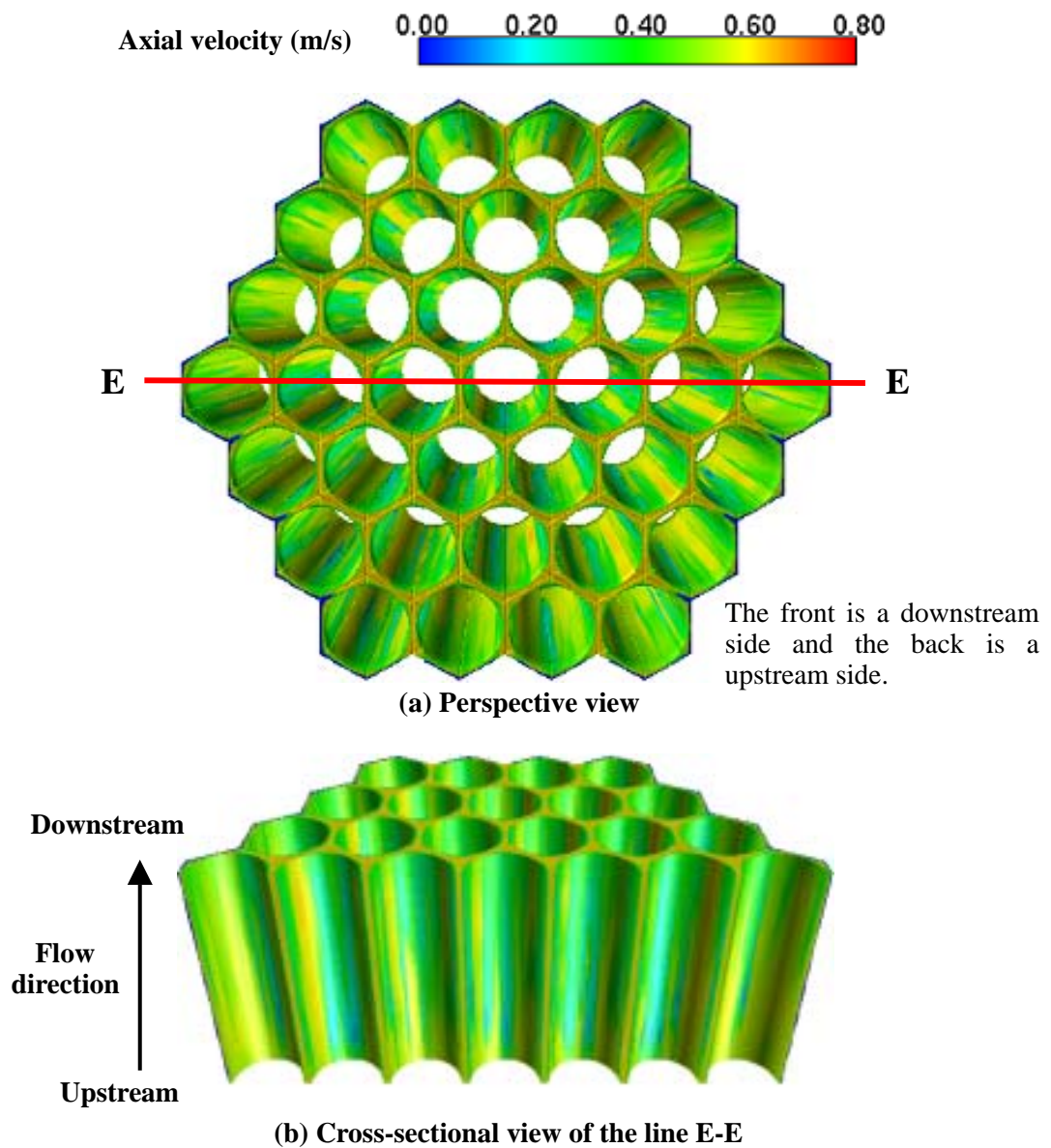


Fig.9 Predicted axial velocity distributions near the position B in Fig.6

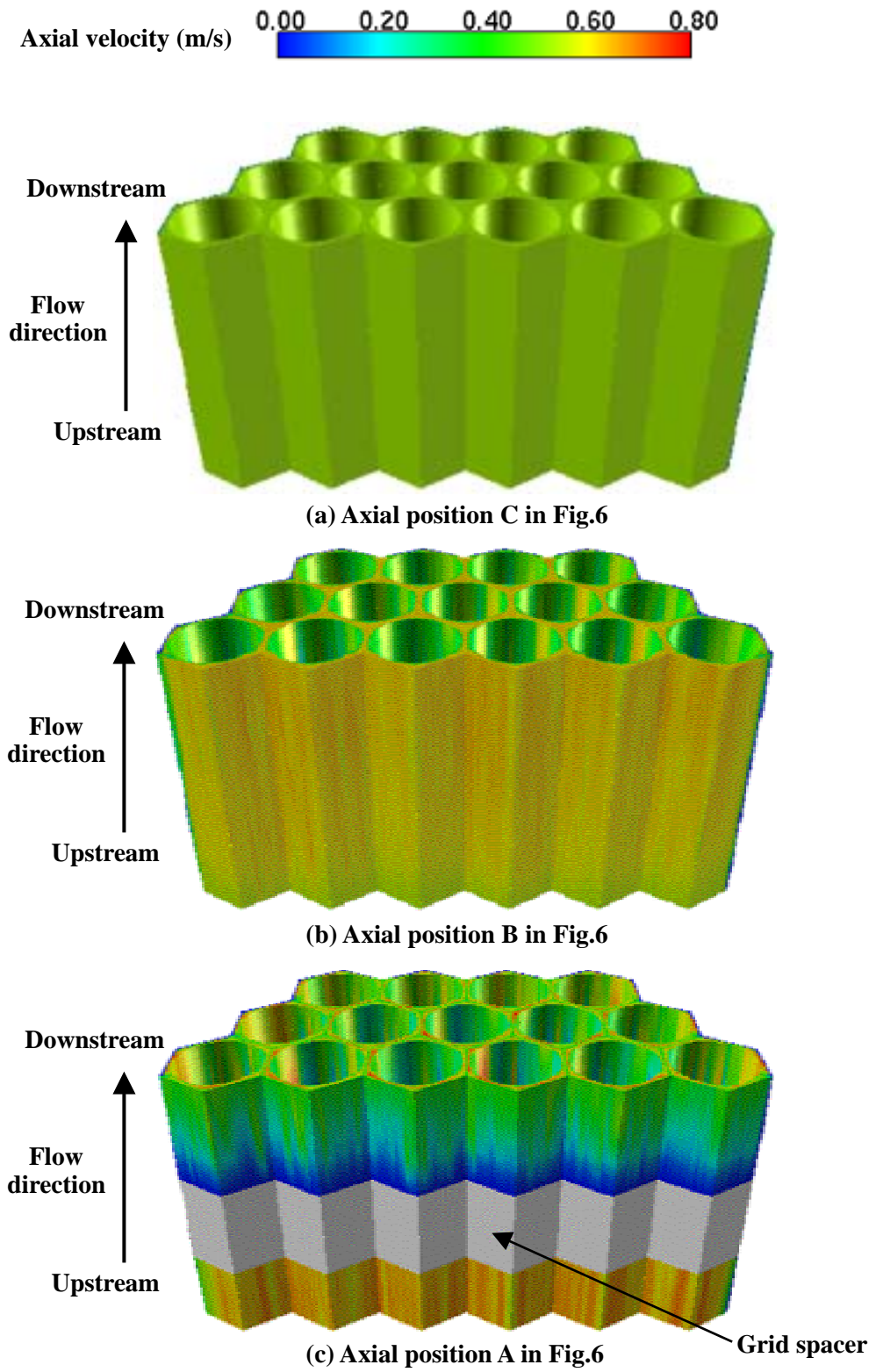


Fig.10 Predicted axial velocity distributions in core flow regions with and without a grid spacer

Predicted axial velocity distributions in the arbitrary regions of a fuel bundle are shown in Fig. 10. Here, Fig. 10 (a) represents the predicted result at the position C in Fig. 6. Similarly, Figs. 10 (b) and (c) show the predicted results at the position B and A in Fig. 6, respectively. The result shown to the front of each figure indicates the axial velocity distribution that is cut to the axial direction at the exact middle position of the gap spacing between fuel rods. The velocity is shown from blue to red using color gradation; as for blue, the velocity shows zero, and, as for red, it shows 0.8 m/s. Fig. 10 (a) shows a predicted result near the channel inlet of a fuel bundle, and the axial velocity is still underdeveloped. The average axial velocity of the whole domain displayed on this figure is about 0.45m/s. In Fig. 10 (b), the axial velocity develops gradually and then produces a distribution between the core flow region and a side wall region. In Fig. 10 (c), the axial velocity distribution differs greatly before and behind the grid spacer position. When there is no grid spacer, a flow progresses almost uniformly. When there is a grid spacer, however, the region in which the axial velocity falls down extremely is formed just behind a grid spacer. Therefore, the axial velocity is expressed with blue just behind a grid spacer as can be seen in Fig. 10 (c).

Conclusion

Fluid flow characteristics in a tight-lattice fuel bundle with grid spacers were analyzed numerically using a newly developed two-phase flow analysis code under the conditions of the full bundle size and non-heated isothermal flow. Conventional analysis methods such as sub-channel codes need composition equations based on the experimental data. In case that there are no experimental data regarding to the thermal-hydraulics in the tight-lattice core, therefore, it is difficult to obtain high prediction accuracy on the thermal design of the RMWR. Then the direct numerical simulations with the earth simulator were chosen. The axial velocity distribution in a fuel bundle changed sharply around a grid spacer and its quantitative evaluation was attained in the present preliminary numerical study. The high prospect was acquired on the possibility of establishment of the thermal design procedure of the RMWR with large-scale direct simulations.

Nomenclature

- D : Substantial time derivative, or fuel rod diameter
- e : Internal energy
- g : Gravity acceleration, or gap spacing between rods
- p : Pressure
- q : Heat source
- T : Temperature
- t : Time, or thickness of a grid spacer
- u : Velocity
- x : Rectangular coordinate
- y : Rectangular Coordinate
- z : Rectangular Coordinate
- Greek symbols
- ϕ : Volume fraction
- λ : Viscosity
- ρ : Density

σ : Surface tension

τ : Stress tensor

Subscripts

g : Gas phase

i, j : Species in multicomponent system

l : Liquid phase

Acknowledgment

The present numerical simulations were carried out using the ES in Japan. The authors would like to express their gratitude to the Earth Simulator Center (ESC) and Prof. Sato who is a director general of the ESC. A special thank is given to Drs. N. Inoue and T. Kano of the center for promotion of computational science and engineering in the JAERI for their support and great cooperation in execution of the ES.

References

- [1] J. E. Kelly, S. P. Kao and M. S. Kazimi, "THERMIT-2: A Two-Fluid Model for Light Water Reactor Subchannel Transient Analysis", MIT-EL-81-014 (1981).
- [2] M. J. Thurgood, "COBRA/TRAC – A Thermal-Hydraulic Code for Transient Analysis of Nuclear Reactor Vessels and Primary Coolant Systems, Equation and Constitutive Models", NUREG/CR-3046, PNL-4385, Vol. 1, R4 (1983).
- [3] S. Sugawara and Y. Miyamoto, "FIDAS: Detailed Subchannel Analysis Code Based on the Three-Fluid and Three-Field Model", Nuclear Engineering and Design, 129, (1990) pp.146-161.
- [4] T. Okubo et al., "Design of Small Reduced-Moderation Water Reactor (RMWR) with Natural Circulation Cooling", Proceedings of International Conference on the New Frontiers of Nuclear Technology; Reactor Physics, Safety and High-Performance Computing (PHYSOR 2002), Seoul, Korea (2002).
- [5] T. Iwamura et al., "Development of Reduced-Moderation Water Reactor (RMWR) for Sustainable Energy Supply", Proceedings of The 13th Pacific Basin Nuclear Conference (PBNC 2002), Shenzhen, China (2002) pp.1631-1637.
- [6] T. Iwamura et al., "Core and System Design of Reduced-Moderation Water Reactor with Passive Safety Features", Proceedings of ICAPP 2002, No.1030, Hollywood, Florida (2002).
- [7] For instance, The Earth Simulator Center, [//www.es.jamstec.go.jp/esc/](http://www.es.jamstec.go.jp/esc/)
- [8] Yoshida, et al., "Numerical Simulation of Liquid Film around Grid Spacer with Interface Tracking Method", GENES4/ANP2003, Kyoto, Japan (2003).
- [9] T. Yabe, et al., "The Constrained Interpolation Profile Method for Multiphase Analysis", J. Comput. Phys., 169-2, (2001) pp.556-593.
- [10] D. L. Youngs, (K. W. Morton and M. J. Baine, Edi.), "Numerical Methods for Fluid Dynamics", Academic Press, (1982) pp.273-285.
- [11] J. U. Brackbill, "A Continuum Method for Modeling Surface-Tension", J. Comput. Phys., 100-2, (1992) pp.335-354.
- [12] A. Ohnishi, et al., "Development of Predictable Technology for Thermal/Hydraulic Performance of Reduced-Moderation Water Reactors (1) – Master Plan –", 2003 JSME Annual Meeting, No.03-1, (2003), [in Japanese].

- [13] M. Kureta, et al., "Development of Predictable Technology for Thermal/Hydraulic Performance of Reduced-Moderation Water Reactors (2) – Large-Scale Thermal/Hydraulic Test and Model Experiment –", 2003 JSME Annual Meeting, No.03-1, (2003), [in Japanese].